energies

MDPI

Article

A Hybrid RCS Reduction Method for Wind Turbines

Shyh-Kuang Ueng

Department of Computer Science & Engineering, National Taiwan Ocean University, Keelung 202, Taiwan; skueng@mail.ntou.edu.tw

Received: 26 June 2020; Accepted: 25 September 2020; Published: 29 September 2020

Abstract: Wind turbine towers produce significant scatterings when illuminated by radars. Their reflectivity affects air traffic control, military surveillance, vessel tracking, and weather data sensing processes. Reducing the radar cross-section (RCS) of wind turbines is an essential task when building wind farms. It has been proved that round and bumpy structures can scatter radar waves and reduce the RCS of a reflector. Other research showed that taper towers generate smaller radar returns than cylindrical towers. In this research, we combine both strategies to devise a more effective method for designing wind turbine towers in the hope that their RCS can be further reduced. The test results reveal that the proposed method out-performs current reshaping methods. Wind turbine towers possessing taper shapes and periodic surface bumps deflect incident electromagnetic waves to insignificant directions. Thus, radar returns in the back-scattering directions decrease. Other experiments also verify that the proposed method maintains its effectiveness for radar waves with varying frequencies and polarization.

Keywords: RCS reduction; wind turbines; reshaping methods

1. Introduction

The massive metallic towers of wind turbines produce significant back scatterings when illuminated by radar waves. Their radar cross-sections (RCS) are larger than those of Boeing 737 airplanes. Thus, wind turbines become a menace to the operations of air and sea traffic control, weather monitoring, and military surveillance radars [1]. This hazard is the top reason for the cancellation of wind farm installations [2]. The study in [2] surveyed the scattering capabilities of all individual components of a wind turbine and concluded that 75% of the radar returns were produced by the tower. If the radiation from the tower is decreased, the entire scattering of the wind turbine is reduced too. Furthermore, the tower is used for supporting the electricity generator, blades, and nacelle. It is a stationary structure and does not rotate as the blades do. Applying RCS alleviation processes upon the tower is more economic and produces almost no negative effects on the electricity generation capacity of the wind turbine. Thus, alleviating radar returns from the tower is the top priority for decreasing the RCS of a wind turbine.

Some strategies have been proposed to reduce the radar returns caused by wind turbine towers. In the work of [3,4], researchers proposed to coat these metallic structures with radar absorption materials (RAM) to weaken their scatterings. RAM methods possess some engineering difficulties. First, the thickness of the coating layer must be properly calculated so that radar waves of a specific frequency can be absorbed. Secondly, RAMs are expensive, and their installation costs are high. Third, their weights increase the load of the tower. Furthermore, the endurance of RAMs is another problem since some wind turbines are installed off-shore and erosion can damage the coatings.

An alternative methodology is to change the shape of the tower to divert incident radar waves toward insignificant directions so that the back scatterings are declined. Based on this rationale, some reshaping methods have been proposed. In the paper of [2], Pinto et al. proposed to shape a wind

turbine tower with tapering effect. The resultant tower has a larger base end and a smaller top end. It has been proved that this tapered tower produces less radar returns than a cylindrical tower when illuminated by S- and X-band radars. In [5], Ling et al. discovered that adding bump structures on the surface of a reflector could effectively divert the reflected EM waves. Their approach was revised by Ueng et al. to lower the RCS of wind turbines [6,7]. In the methods of [6,7], the surfaces of wind turbine towers are augmented with horizontal or vertical periodic bumps to scatter incident radar waves. Hence, radar returns from wind turbine towers are alleviated. The authors also published and analyzed simulation results and verified that bumps in specific densities and heights significantly reduce RCS of wind turbine towers. In a more recent work [8], Ueng and Chen proposed to combine the two reshaping strategies of [2,6,7] to design a more efficient RCS reduction method. However, a pragmatic algorithm for building wind turbine towers was absent from their paper.

Besides reshaping and RAM methods, some researchers proposed to use metasurfaces for RCS reduction. In their methods, layers of metallic and dielectric slabs are adhered in specific arrangements. The thicknesses and covering areas of these slabs are carefully selected to produce out-of-phase effects in the reflected radar waves. Thus, the RCS of the surface is reduced because of the destructive interferences between reflected beams [9]. In a similar search, Song et al. designed a hybrid RCS alleviation method [10]. They created a graphene sheet upon the target surface. The space between the graphene sheet and the target surface was filled with foams. Then, they attached grating structures on the graphene sheet. As radar waves reach the target, the graphene layer absorbs some energy from the incoming waves and the grating structures generate high order reflections to reduce the back scatterings. In the work of [11,12], scientists employed artificial magnetic conductors (AMC) to weaken the RCS of metallic surfaces. In these methods, specially designed AMC cells are designed and fabricated on metallic surfaces. These AMC cells form a chessboard pattern. As metallic surfaces are illuminated by radar waves, the ACM cells diversify the phase distribution of the reflected beams and generate phase-cancellation effects. Thus, the RCS of the target is decreased. These methods do not modify the shape of the target. However, they share some weaknesses with RAM methods. Their costs are relatively high and the endurance of the coating layers in harsh environments is questionable.

In this research, we adopt the idea of [8] and develop an innovative reshaping method aiming to design wind turbine towers producing a smaller RCS. Our method combines the tapering effect method of [2] and the bump surface methods of [5–7] to model wind turbine towers. The resultant towers possess tapered shapes and periodic surface bumps. Besides devising and formulating our reshaping approach, numerous simulations have also been carried out to study the effectiveness of the proposed method. The collected results show that our hybrid reshaping method is superior to those previous reshaping methods presented in [2,5–7]. Furthermore, the achieved RCS reduction exceeds the combination of the individual reshaping methods. Other experiments show that the proposed strategy is applicable for a wide range of frequencies and different radar wave polarizations. Thus, it can be used to decrease scatterings for various radar systems. We also conduct simulations to find the optimal tapering angles and to study the combined effect of taper ratio and radar frequency upon the proposed reshaping strategy. The results are also presented and analyzed in this article.

2. Materials and Methods

As the proposed RCS reduction method is a hybrid reshaping strategy, the resultant towers possess tapered shapes and surface bumps. There are fine structures on the towers' surfaces, and the taper ratio of each individual tower may be different. Instead of designing these towers manually by using geometric modelling tools, we deduce mathematic formulas to model them. The bump density, bump height, bump direction, and taper ratio are regarded as control parameters in the formulas. Thus, by altering these variables, towers with different appearances can be automatically created to comply with the requirements of the users.

2.1. Cylindrical, Taper, Bump, and Bamboo Tower Modelling

The reshaping methods for modelling towers with bumpy and tapering effects have been presented in [5–7]. Based on these reshaping methods, we developed new geometrical formulations to create hybrid towers. For the sake of completeness, the reshaping methods of [5–7] will be first introduced in this subsection. The newly developed modeling algorithms for the hybrid towers is presented in Section 2.2.

Our reshaping algorithm uses a cylinder tower as the template. Then, by deforming the cylindrical tower, other types of towers are constructed. In this subsection, we will present the proposed modelling formula step by step and case by case. We assume that, in the world coordinate system, the x- and y-axes span the horizontal plane while the z-axis points vertically, and the height and radius of the cylindrical tower are h and r. Then, the coordinates of all points on the cylindrical tower surface can generated by the following formula:

$$\begin{array}{c} x = r\cos(\alpha), \\ y = r\sin(\alpha), \\ \frac{-h}{2} \le z \le \frac{h}{2}, \end{array} \tag{1}$$

where α ranges from 0 to 2π. An image containing a cylindrical tower and the world coordinate system is shown in Figure 1a.

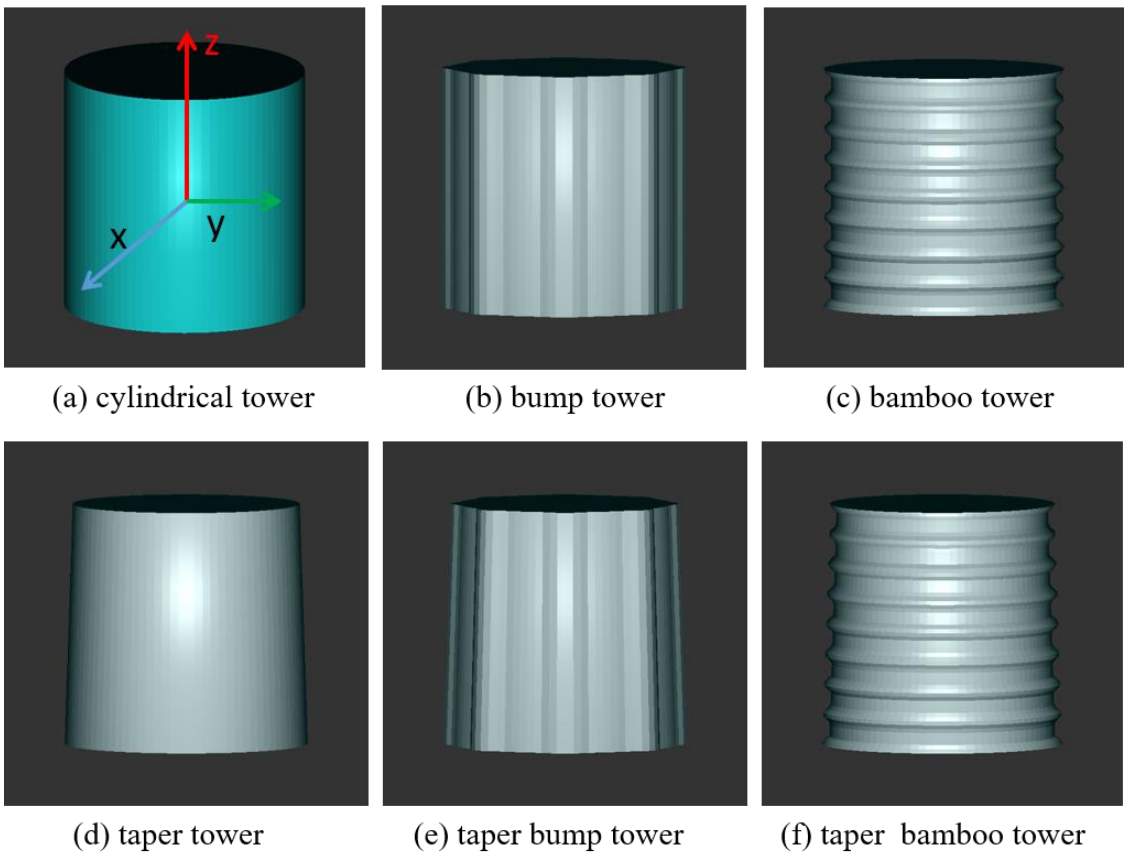

Figure 1. Wind turbine towers. Upper row, towers without tapering effect; lower row: towers with tapering effect.

Based on Equation (1), we deduced a method to construct a tapered tower, assuming that the radii of the bottom end and the top end of the tapered tower are r_B and r_T. The slope, i.e., the taper ratio, of the tower surface is defined as:

$$T = \frac{r_B - r_T}{h}. \tag{2}$$

The radius of the tapered tower varies with the z-coordinate and can be expressed as a function of z-coordinate:

$$r(z) = r_B - T * (z + \frac{h}{2}). \tag{3}$$

By substituting $r(z)$ of Equation (3) into Equation (1), we can generate a tapered tower with a taper ratio T. An example taper tower is displayed in Figure 1d.

By adding perturbations to the x- and y-coordinates in Equation (1), we can generate bumps on a cylindrical tower's surface. These perturbations come from a wave function $D(\alpha)$, which is defined as follows:

$$D(\alpha) = A\cos(k\alpha), \tag{4}$$

where A and k are the amplitude and wave number of this wave function, respectively, and α ranges from 0 to 2π. Then, the x- and y-coordinates of the tower surface can be modelled by using the following equation:

$$\begin{aligned} x(z,\alpha) &= (D(\alpha) + r)\cos(\alpha), \\ y(z,\alpha) &= (D(\alpha) + r)\sin(\alpha). \end{aligned} \tag{5}$$

In Equation (5), the perturbation function alters the radius of the tower and transforms the tower surface into a wavy surface. The crests divert incoming radar rays and reduce the RCS of the tower. However, the troughs resemble parabolic reflectors. They may concentrate incident radar rays and produce significant back scatterings. To preserve the crests and eliminate the troughs, we put the following constraint upon $D(\alpha)$:

$$D(\alpha) = \max(A\cos(k\alpha), 0). \tag{6}$$

Subsequently, D becomes a non-negative periodic function of α and generates a sequence of convex bumps around the tower surface. The tower is named as the bump tower in this article. A bump tower is shown in Figure 1b. The bumps are parallel to the z-direction.

By revising the periodic function D, we can reorient the bumps by 90 degrees and add equal-spaced rings on the tower surface. Assuming that k rings are to be produced, the inter-ring space is computed by

$$\lambda = \frac{h}{k}. \tag{7}$$

By using λ, we redefine D as a function of the z-coordinate:

$$D(z) = \max(A\cos(\frac{2\pi z}{\lambda}), 0). \tag{8}$$

Consequently, D becomes a periodic and non-negative function of z-coordinate. By substituting D of Equation (8) into Equation (5), the x- and y-coordinates of the tower surface are computed as below:

$$\begin{aligned} x(z,\alpha) &= (D(z) + r)\cos(\alpha), \\ y(z,\alpha) &= (D(z) + r)\sin(\alpha). \end{aligned} \tag{9}$$

Since the tower possesses a series of convex rings and resembles a bamboo, we call it the bamboo tower in this article. The image of a bamboo tower is contained in Figure 1c. Its surface contains horizontal rings which are expected to reflect incident radar waves to the ground and the sky.

2.2. Hybrid Tower Modelling

It has been proved that towers possessing surface bumps or taper shapes produce less RCS than cylindrical towers [2,5–7]. A reshaping method which combines both strategies would be of great values to us. However, to our knowledge, no study has been carried out to investigate the RCS reduction capability using both methods at the same time. Thus, we created two types of hybrid towers

which have surface bumps and tapering shapes in hope to further alleviate back scatterings from wind turbine towers.

First, we mixed the bump tower with the taper tower to create a taper bump tower. To achieve this goal, we deduced the following function to control the radius r of the tower:

$$\begin{array}{l} r(\alpha, z) = (r_B + D(\alpha)) - T * (z + \frac{h}{2}), \\ -h/2 \le z \le h/2, \\ 0 \le \alpha \le 2\pi, \end{array} \tag{10}$$

where T and $D(\alpha)$ are defined in Equations (2) and (6), respectively. Thus, the radius is maximized at the base and linearly decreases along with the z-coordinate. Furthermore, the radius is disturbed by the periodic function D in each cross-section of the tower to create convex bumps. By using the radius function $r(\alpha, z)$, the x- and y-coordinates of the tower surface are modelled by

$$\begin{array}{l} x(\alpha, z) = r(\alpha, z) * \cos(\alpha), \\ y(\alpha, z) = r(\alpha, z) * \sin(\alpha). \end{array} \tag{11}$$

The image of a taper bump tower is displayed in Figure 1e. As the image shows, the tower has a taper shape and a sequence of bumps surrounding its surface.

Then, by using Equations (7) and (8), we vary the radius along with the z-coordinate

$$\begin{array}{l} r(\alpha, z) = (r_B + D(z)) - T * (z + \frac{h}{2}), \\ -h/2 \le z \le h/2, \\ 0 \le \alpha \le 2\pi, \end{array} \tag{12}$$

The radius fluctuates with the z-coordinate and linearly shrinks as the z-coordinate increases. Then, the x- and y-coordinates of the tower surface are calculated by:

$$\begin{array}{l} x(\alpha, z) = r(\alpha, z) * \cos(\alpha), \\ y(\alpha, z) = r(\alpha, z) * \sin(\alpha). \end{array} \tag{13}$$

The resultant tower is called the taper bamboo tower in the following context. An image of the tapered bamboo tower is displayed in Figure 1f. This tower has a tapering shape as well as horizontal convex rings on its surface.

3. Results

Several sets of experiments were conducted to evaluate the proposed reshaping methods. In the first set of tests, we computed the RCS values of the wind turbine towers mentioned in the previous section. Then, we analyzed the test results to find out effective tower shapes. In the second set of experiments, we studied how taper ratio and radar frequency affected the RCS of these towers. The efficiencies of these towers, when illuminated by radar waves of various frequencies, were also compared. In the third set of simulations, we polarized the radar waves both vertically and horizontally and then computed the RCS of these towers. These simulations reveal the influence of polarization upon the performances of the proposed reshaping methods.

In order to save costs, all the experiments were carried out using a simulation program. We used the geometric modelling methods presented in Section 2 to construct virtual wind turbine towers, including a cylindrical tower, a bump tower, a bamboo tower, a taper tower, a taper bump tower, and a taper bamboo tower. The origin of the world coordinate system is located at the tower centers, as shown in Figure 1a. To speed up the computations, the tower height was truncated to six meters. Initial geometrical parameters of the reshaping procedures are listed in Table 1. The radii of the towers were 1.5 m. The taper ratios of the taper tower, the taper bump tower, and the bamboo tower are 0.4/60. Eight bumps were created on the surfaces of the bump tower, the bamboo tower, and the two hybrid

towers. The bump height was 0.1 m. These data represent default values of the geometric parameters but may be changed in experiments to enhance specific effects and tower characteristics.

Table 1. Geometric parameters of the towers.

Base Radius	Number of Bumps	Bump Height	Taper Ratio
1.5 m	8	0.1 m	0.4/60

Unlike RAM methods, the total energy of scattering is not reduced in reshaping methods. The RCS of a target declines because most of the reflected rays are guided to unimportant directions and less energy is sent back toward the transmitting antenna. Evaluating the effectiveness of towers based on their mono-static RCS may result in missing key features of individual reshaping strategies. In this research, we used bi-static RCS to manifest the diversification of energy caused by the tapering effect and bumps. Thus, the characteristics of the towers were better revealed. Furthermore, scatterings in all directions may cause multiple interactions among nearby wind turbines or other objects and interfere radar operations. If the bi-static RCS is decreased, multiple interactions can be alleviated. Therefore, we rely on bi-static RCS to analyze the performances of towers.

3.1. Effectiveness of Hybrid Towers

In the first set of experiments, bi-static RCS values of the hybrid towers were computed. The fundamental radar parameters are depicted in Table 2. The radar was located at the x-axis and was 3000 m away from the origin. Hence, the zenith angle θ of the incident radar waves was 90 degrees while the azimuth angle ϕ of the incident radar waves was zero degrees. One hundred and eighty-one receivers were used to sense scatterings from towers. These receivers were evenly distributed in the boundary of a semicircle. This semicircle was located on the xy-plane and has a radius of 3000 m. The zenith and azimuth angles of these receivers were $\theta = 90°$ and $-90° \leq \phi \leq 90°$. A computer program based on the shooting and bouncing rays (SBR) method [5,13] was employed to compute the RCS of these towers. In the evaluation process, the RCS of the cylinder tower was served as the baseline to verify the efficiencies of the hybrid towers.

Table 2. Radar parameters.

Frequency	Polarization	Radar Distance	Incident Angle
3.0 GHz	H/H	3000 m	$\theta = 90°$, $\phi = 0°$ (x-axis)

3.1.1. Effectiveness of the Tapered Bump Tower

The RCS values of the cylinder tower, the bump tower, the taper tower, and the taper bump tower are displayed in Figure 2. The RCS of the cylinder tower is rendered in green color and used as the baseline. The RCS values of the bump tower, taper tower, and the taper bump tower are shaded in red color. In the left part, the bi-static RCS values of the cylinder tower and the bump tower are depicted. The bump tower produced less RCS around the backscattering directions ($\theta = 90°$, $-20° \leq \phi \leq 20°$). The difference is about 5 dB. In the middle part, the RCS values of the cylinder tower and the taper tower are rendered. The taper tower reduced the radar returns by 10 dB around the backscattering directions. The RCS of the taper bump tower is shown in the right part. This hybrid tower reduced the RCS value by about 20 dB in the backscattering directions. The results show that the taper bump tower is superior to the bump tower and the taper tower. It produces additive improvement. The reduction in RCS gained by the taper bump tower exceeds the sum of the RCS reductions contributed by the taper tower and the bump tower.

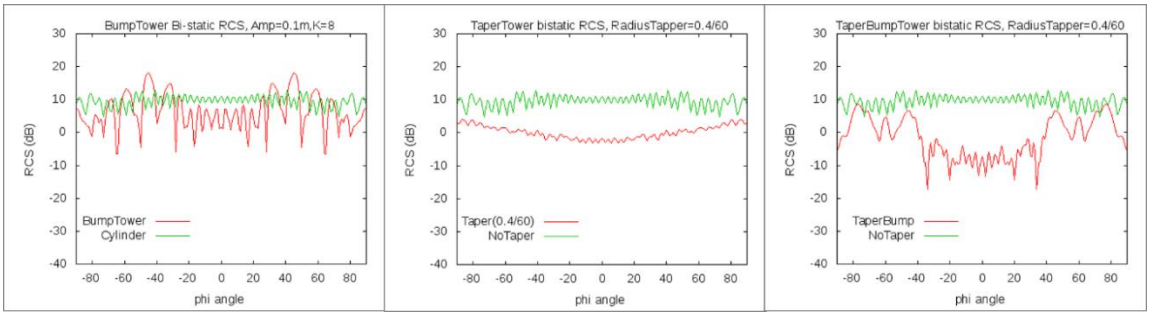

Figure 2. (**Left**) radar cross-section (RCS) of the bump tower. (**Middle**) RCS of the taper tower. (**Right**) RCS of the taper bump tower. RCS of the cylinder tower is rendered in green color and used as the baseline.

The bump tower and taper bump tower generated stronger scatterings around the directions $-70^{\circ} \leq \phi \leq -50^{\circ}$ and $50^{\circ} \leq \phi \leq 70^{\circ}$ and deteriorated their performances. The incident angle of the radar waves is $\phi = 0^{\circ}$. After hitting the bumps, their reflections concentrate within these two ranges. Thus, the bistatic RCS at these directions is worsened.

3.1.2. Effectiveness of the Tapered Bamboo Tower

The bi-static RCS values of the taper bamboo tower are displayed in the right part of Figure 3. For reference, the bi-static RCS values of the bamboo tower and taper tower are shown in the left and middle parts of the same figure. The bamboo tower and the taper could reduce the back scatterings by 10 dB. However, the taper bamboo tower reduced the RCS value by 20 dB. Thus, the hybrid reshaping method is superior to the other two towers.

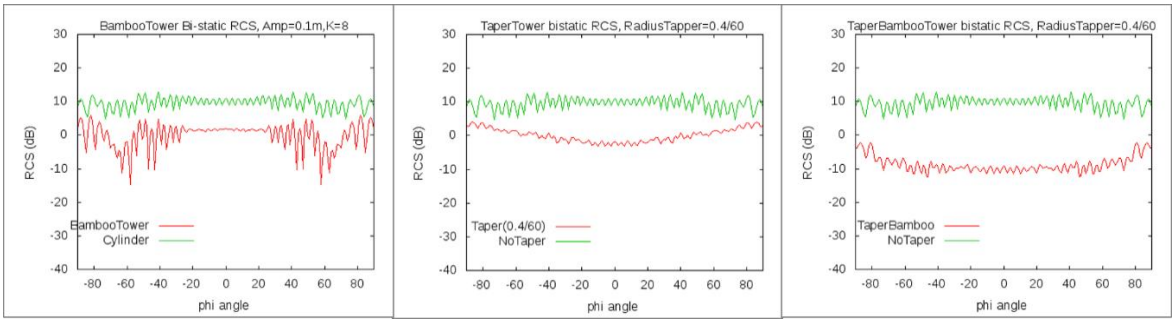

Figure 3. (**Left**) RCS of the bamboo tower. (**Middle**) RCS of the taper tower. (**Right**) RCS of the taper bamboo tower.

Comparing the RCS of the taper bump tower and the taper bamboo tower, we find that the taper bamboo tower can alleviate scatterings in all the azimuth angles. This phenomenon also appears in the RCS of the bamboo tower. We believe that the taper bamboo tower inherits this property from the bamboo tower. Its horizontal bumps scatter the incident radar waves toward the sky and the ground and decrease the bi-static RCS in all azimuth angles.

3.2. Taper Ratio and RCS

If we fix the radius of the tower base, the shape of a tower is decided by the bump height, bump density, bump direction (vertical or horizontal), and taper ratio. Thus, there are four parameters for modelling a tower. The influence of the bump height and bump density on RCS has been reported in the previous research of [6]. The results showed that a feasible bump height for bump towers should be within 0.1 and 0.9 of the radar wavelength. On the other hand, the most effective bump height for bamboo towers is about 0.2~1.4 times that of the radar wavelength. If the bumps are too short,

they cannot effectively scatter the incident radar waves. However, if the bumps are too high, the bump bases and the tower surface form corners, which produce significant back-scatterings and enhance RCS.

The reasonable number of bumps is usually between four and eight. Bumps reflect radar waves toward insignificant directions. As the number of bumps increases, the radar returns are gradually weakened. Nonetheless, if the bump density is too high, the space between two bumps resembles a concave reflector and generates a strong reflection toward the receivers, thus, RCS increases. Extra experiment results, analysis, and explanation have been presented in the paper of [6]. Thus, these two factors, bump height and density, will not be investigated in this work. Instead, this research focuses on the influences of taper ratio and bump direction on RCS alleviation. High frequency electromagnetic waves carry higher energies and enhance scatterings [7,9]. Furthermore, their wavelengths are shorter and so they can interact with fine structures on tower surfaces more effectively and produce complicated reflections. Thus, the relationship between radar frequency and RCS will also be studied in the tests.

In preparation for the tests, we varied the taper ratio to create towers. The radar distance, polarization, and direction were not altered, though the radar frequency was varied in the simulations. The RCS of each tower was calculated by using the SBR program mentioned above. In each simulation, this program computed bi-static RCS values in all 181 azimuth directions. To emphasize the backscattering strength, we computed the average value of the bi-static RCS within the range of $-20^\circ \leq \phi \leq 20^\circ$ and used it to evaluate the performances of the towers. Though we did not take RCS in all directions into account, this range of azimuth angles covers the major back scatterings sensed by a mono-static radar. Thus, the average radar return of this range is a reasonable measurement for comparing the efficiencies of the towers.

3.2.1. Fixed Radar Frequency

To uncover the relation between taper ratio and RCS, we created five taper towers with taper ratios of 0.2/60, 0.4/60, 0.6/60, 0.8/60, and 1.0/60. Then, we computed their RCS by using the SBR program. The settings of the simulation were the same as those tests in Section 3.1. The results are illustrated in Figure 4. The green curves represent the RCS of the cylinder tower while the red curves show the RCS of these tapered towers. By examining these five results, we found that the higher the taper ratio, the lower the RCS. Therefore, to alleviate radar returns, we should build towers with high taper ratios.

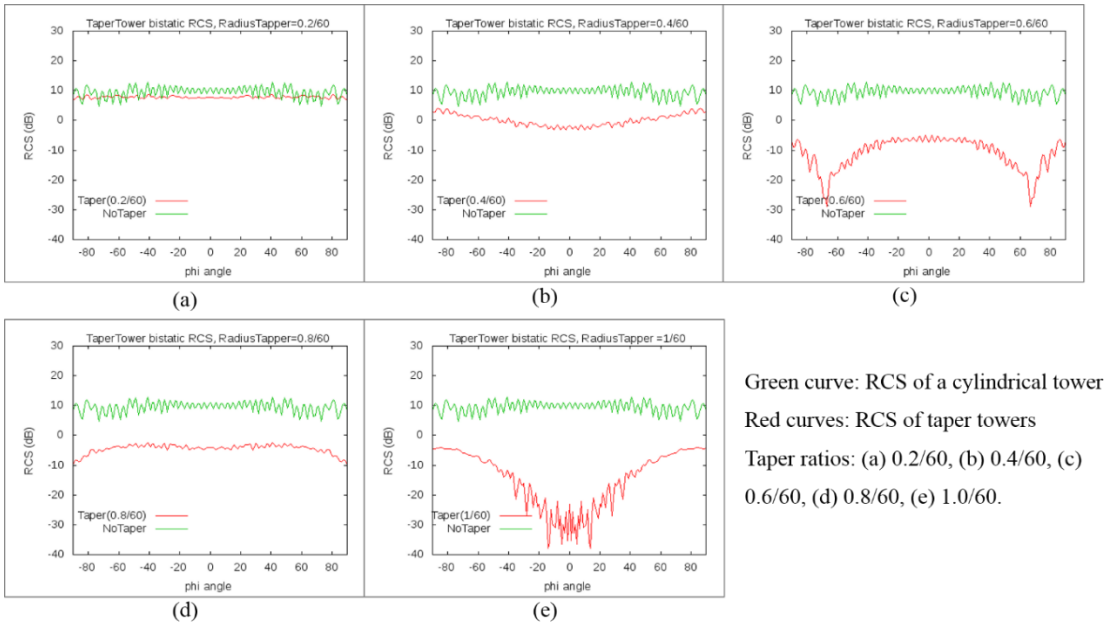

Figure 4. RCS of taper towers with (**a**) 0.2/60, (**b**) 0.4/60, (**c**) 0.6/60, (**d**) 0.8/60, and (**e**) 1.0/60 taper ratios.

However, if the taper ratio is 1/60, the difference of diameter between the top and base ends in a 60-m-tall tower is two meters. If the diameter of the top end is three meters, the diameter of the base end will be five meters. Fixing the size of the top end and increasing the taper ratio will widen the difference and the taper tower will have a very large base. In the aspect of building costs, this tower will become impractical. Thus, we suggest that the taper ratio should not exceed 1/60.

3.2.2. Varied Radar Frequency

In following tests, we studied the influence of radar frequency on the RCS of towers. At first, we created six taper towers, six taper bump towers, and six taper bamboo towers. The taper ratios of these towers were 0.0/60, 0.7/60, 1.1/60, 1.3/60, and 1.5/60, respectively. Then, we illuminated each tower by using radar waves of six different radar frequencies (1~6 GHz). The average bi-static RCS of the directions, $\theta = 90°$ and $-20° \leq \phi \leq 20°$, were calculated and used as the metrics for comparisons.

The results are illustrated in Figure 5. The RCS of towers with a 0.0/60 taper ratio is represented by red curves. The RCS of other towers are rendered in green, blue, purple, cyan, and brown colors. In part (a), the test results of the taper towers are displayed. As the image shows, the RCS of the taper tower with a 0.0/60 taper ratio increased along with the radar frequency. On the other hand, the RCS values of other taper towers slightly decreased as the radar frequency increases. Higher frequency radar waves are more similar to light rays than lower frequency radar waves. Scatterings caused by the tapering surfaces become important, and thus more energy of the incident electromagnetic waves is reflected toward insignificant directions.

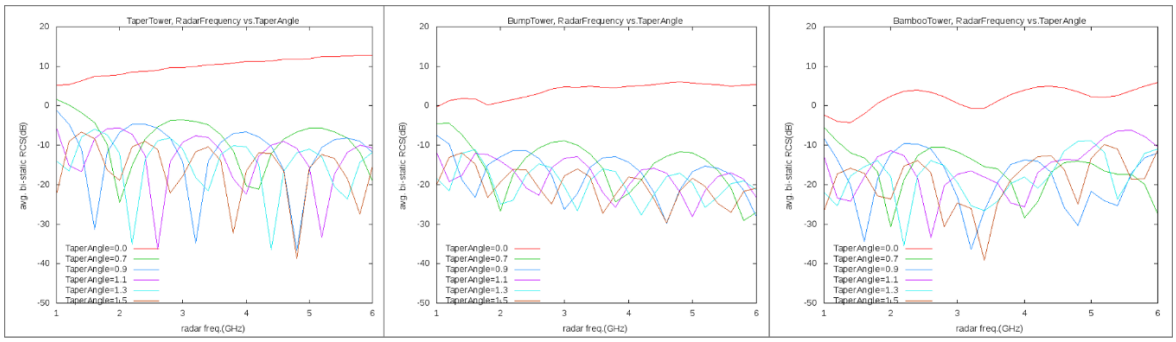

(a) Taper towers (b) Taper bump towers (c) Taper bamboo towers

Figure 5. Average bi-static RCS of (**a**) taper towers, (**b**) taper bump towers, and (**c**) taper bamboo towers. Radar frequency: 1~6 GHz, taper ratios: 0.0/60~1.5/60.

The simulation results reveal that taper bump towers and taper towers are effective in reducing RCS. However, taper bump towers generate a lower RCS than taper towers. The bumps on their surfaces help to scatter more energies of the incident electromagnetic waves. Hence, their RCS is further decreased. The RCS of the taper bamboo towers are presented in part (c) of Figure 5. As the radar frequency increases from 1 GHz to 3 GHz, their RCS values decrease. Then, their RCS magnitudes increase as the radar frequency increases. This phenomenon is more obvious for taper bamboo towers with higher taper ratios. In the taper bamboo towers, the bumps are horizontal rings. As the taper ratio increases, the reflections from one ring will be further reflected by neighboring rings and cannot be directed to the sky or the ground straightly. Thus, more energy is sensed by the receivers. As the radar frequency exceeds 4 GHz, these scatterings become more important and the RCS of the bamboo towers are enlarged.

3.3. Tower Type and RCS

In another study, we compared the performances of taper towers, taper bump towers, and taper bamboo towers. The simulation settings and measurement metrics were the same as the previous

experiments. The results are depicted in Figure 6. The RCS of the taper towers, the taper bump towers, and the taper bamboo towers are represented by the red, green, and blue curves, respectively.

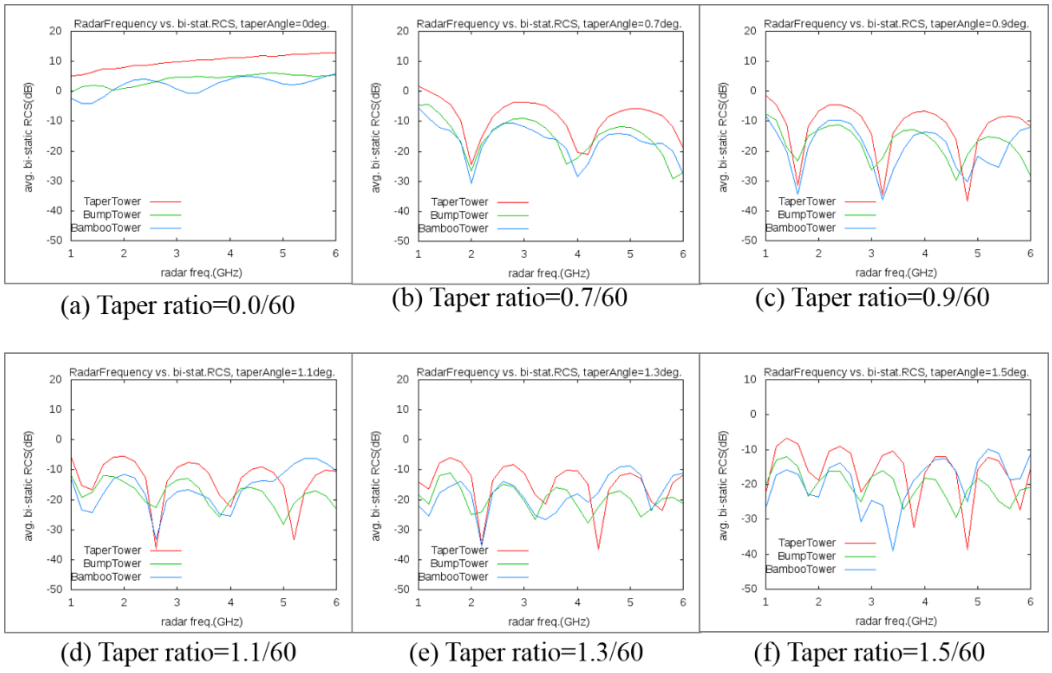

(a) Taper ratio=0.0/60 (b) Taper ratio=0.7/60 (c) Taper ratio=0.9/60

(d) Taper ratio=1.1/60 (e) Taper ratio=1.3/60 (f) Taper ratio=1.5/60

Figure 6. RCS of taper, taper bump, and taper bamboo towers under different radar frequencies and taper ratios. Red, taper towers; green, taper bump towers; blue, taper bamboo towers.

As the results show, taper bamboo towers outperform taper towers and taper bump towers if the taper ratio is less than or equal to 0.7/60. However, as the pater ratio exceeds 1.1/60, the effectiveness of taper bamboo towers deteriorates, especially for higher radar frequencies. In these cases, taper bump towers are the best reshaping method for the RCS reduction process. This result verifies the analysis presented in Section 3.2.2. As the radar frequency increases, the radar waves resemble planar light rays. The inter-ring reflections enlarge the back scatterings and damage the performance of the taper bamboo towers.

3.4. Radar Frequency and RCS

The results presented in Section 3.3 show that taper bamboo towers become less effective on alleviating average bi-static RCS as the radar frequency increases. To further study the influence of radar frequency upon the proposed reshaping methods, we performed another set of tests. In the simulations, the initial radar frequency was 1.0 GHz. Then, the radar frequency was gradually increased until it reached 10.0 GHz. The incremental value was 0.25 GHz. The taper ratios were set to 0.4/60, 0.7/60, 1.4/60, and 1.8/60, respectively. The number of bumps on the tower surfaces was decreased to six. Thus, the gaps between bumps were widened to prevent the creation of cavities. However, the bump height was increased to 10 cm to enhance scatterings. There were four towers used in this study, including a cylinder tower, a taper tower, a taper bump tower, and a taper bamboo tower.

The tests results are plotted in Figure 7. The average bi-static RCS of the cylinder, taper, taper bump, and taper bamboo tower are drawn in purple, green, blue, and yellow color, respectively. For lower taper ratios, 0.4/60 and 0.7/60, the taper bamboo tower is the most effective tower for reducing back scatterings. Nonetheless, as the taper ratio increases, its performance decreases. It generates peak average bi-static RCS at some radar frequencies. For taper ratio equals to 1.0/60, 1.4/60, and 1.8/60, the peak RCS occurs at the radar frequencies of 9.0 GHz, 6.5 GHz, and 5.0 GHz, respectively. We conjecture that the sudden increasing of average bi-static RCS is caused by the coupling effects of radar wavelength, taper ratio, and bump height. In this set of tests, the bump height was 10 cm.

The radar frequency, causing peak average bi-static RCS, decreased as the taper ratio increases. A similar phenomenon can be found in the results of Figure 6d–f, though the bump height is shorter, 8 cm, in these simulations. The magnitude of the peak average RCS is smaller.

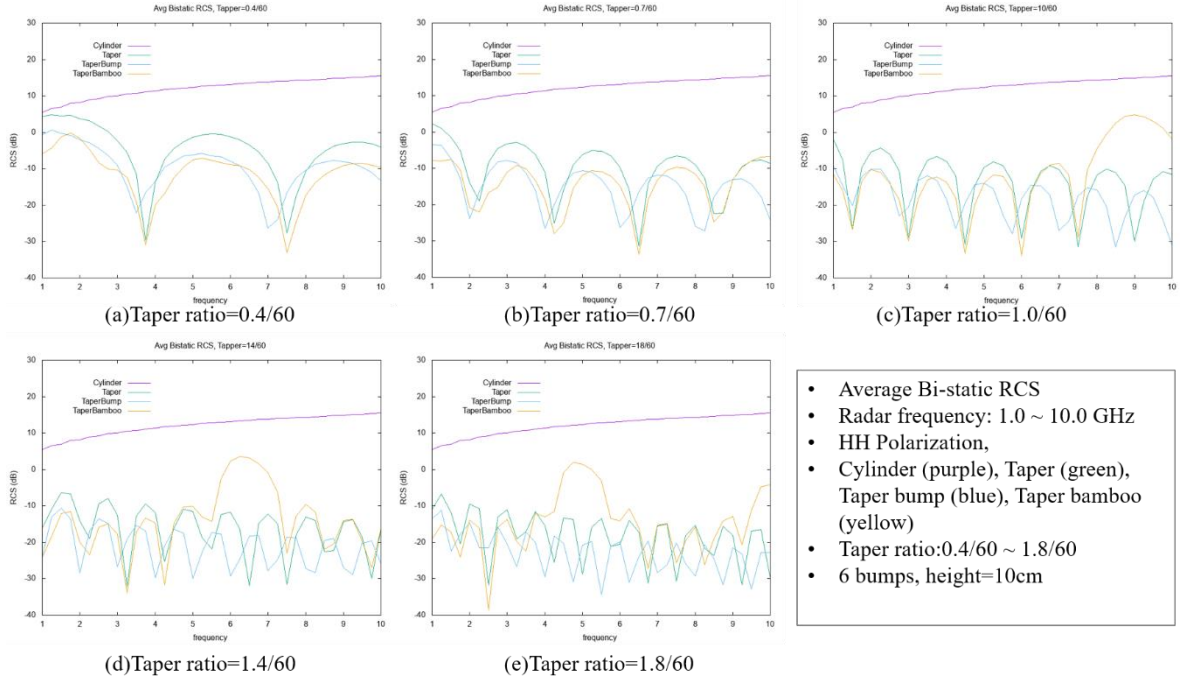

Figure 7. Average RCS of cylinder, taper, taper bump, and taper bamboo towers illuminated by radar with 1.0~10.0 frequencies.

The average bi-static RCS of the taper and taper bump tower fluctuate with radar frequency. The fluctuation becomes more frequently as the taper ratio grows. Globally, their efficiencies improve as the taper ratio and radar frequency increase. These two towers offer stable RCS reductions for all the radar frequencies and taper ratios. It is hard to compare their performances because of the fluctuation. However, in general, the taper bump tower is superior to the taper tower.

3.5. Polarization and RCS

In the previous computations, the radar waves were horizontally polarized. In order to explore the influence of polarization, we computed the RCS of towers by using not only HH but also VV polarization in another set of the experiments. The testing models included cylinder, taper, taper bump, and taper bamboo towers. The geometric parameters were fixed as follows: the taper ratio was 1.0/60; the number of bumps was six; and the bump height was 10 cm. Nonetheless, the radar frequency was set to 3, 6, and 9 GHz to study the combined effect of radar frequency and polarization. The directions and locations of the radar and the receivers were the same as the settings in Section 3.1.

The performances of the towers were evaluated by using their bi-static RCS. The bi-static RCS of the HH and VV polarization are shown in Figures 8 and 9. The bi-static RCS of the cylinder, taper, taper bump, and taper bamboo towers are rendered in purple, green, blue, and yellow color, respectively. These figures show that the bi-static RCS under HH and VV polarization are similar, especially for the cylinder, taper, and taper bamboo tower. Only the bi-static RCS of the taper bump tower are affected by the polarization method. To uncover the difference, we draw the HH and VV bi-static RCS of the taper bump tower in Figure 10. The data obtained by using HH- and VV-polarization are shaded in purple and green curves. The RCS of HH-polarization is better than that of the VV-polarization for radar frequencies equal to 3 and 9 GHz. However, the difference is not significant within the major back-scattering directions, $-20^{\circ} \leq \phi \leq 20^{\circ}$.

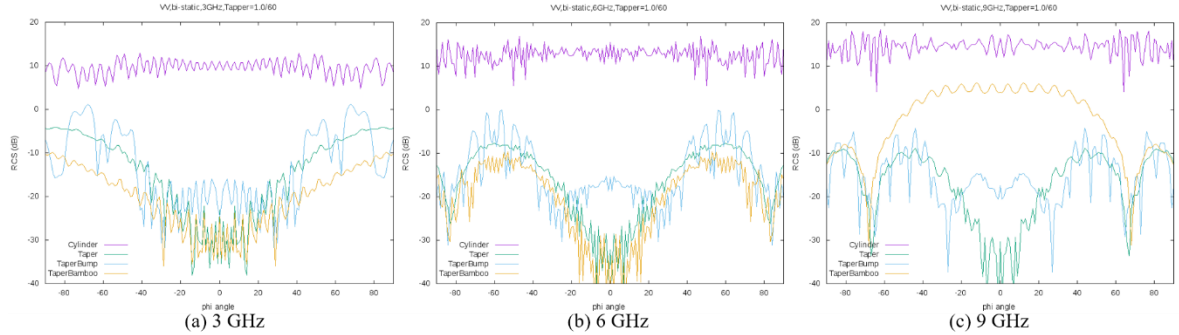

(a) 3 GHz (b) 6 GHz (c) 9 GHz

Figure 8. Bi-static RCS of the cylinder, taper, taper bump, and taper bamboo towers, illuminated by VV-polarized radar waves.

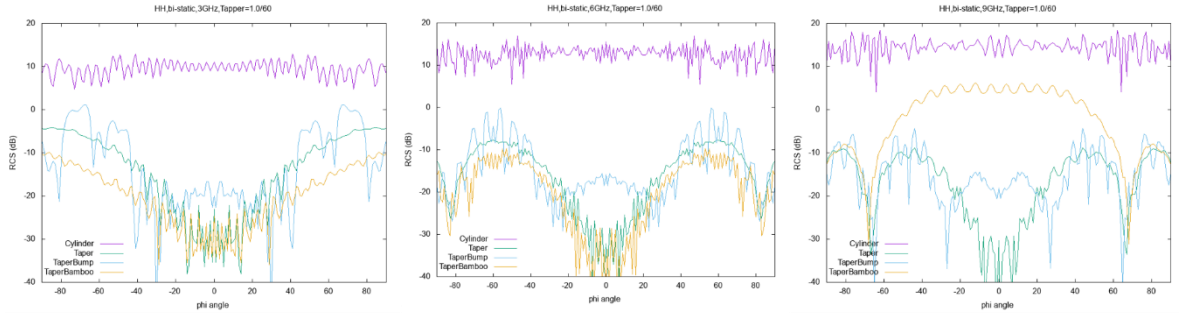

(a) 3 GHz (b) 6 GHz (c) 9 GHz

Figure 9. Bi-static RCS of the cylinder, taper, taper bump, and taper bamboo tower, illuminated by HH-polarized radar waves.

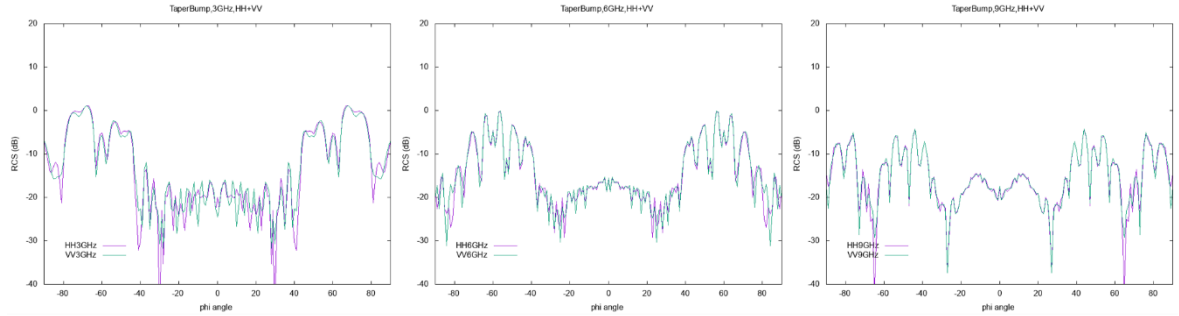

(a) 3GHz (b) 6GHz (c) 9GHz

Figure 10. Bi-static RCS of the taper bump tower illuminated by HH- and VV-polarized radar waves. The purple and green curve represent HH- and VV-polarization bi-static RCS.

3.6. Discussion

In the experiments, the heights of the targets were relatively short compared with real wind turbine towers. The RCS values cannot be used to represent the radar returns of wind turbine towers. Since the main themes of this research focus on developing reshaping methods and studying the effectiveness of the proposed RCS reduction strategies, computing the RCS of a wind turbine is out of the scope of this research. However, assuming a tower is divided into N sections, the RCS values of the tower can be computed as follows:

$$B_\theta = \sum_{i=1}^{N} B_i \,, \tag{14}$$

where B_i is the RCS of the i-th section.

In the experiments, the incident radar waves travelled horizontally at $\theta = 90$. Their direction was orthogonal to the z-axis and parallel with the xy-plane. In reality, radar waves may hit the wind

turbines at smaller zenith angles if the radar is located at higher altitudes and shorter distances. In our reshaping methods, the top end of each individual tower was modelled as a flat surface. If we decrease the zenith angle, some of the rays will hit the top end and produce radar returns. This reflectivity will be included in the resultant RCS values and obscure the contributions produced by the tapering effect and bumps. In order to prevent this problem, the zenith angle was fixed at $\theta = 90$ in this study.

The bumps on the surface of a tower cause extra drag forces and increase the load of the tower. However, these structures enhance the mechanical strength of the tower (similar effects can be found on bamboos and tall man-made buildings). Towers can bear the added load and drag forces. In the reshaping methods, the bumps resemble waves without crests. We can generate a bumpy tower by using a flat metal sheet. At first, we press the sheet to produce vertical or horizontal bumps on the sheet surface. Then, we roll the sheet to form a bumpy tower.

4. Conclusions

Bumps and tapering effects are efficient strategies for reducing the RCS of wind turbine towers. When separately applied on the towers, each of these approaches is capable of decreasing radar returns. In this research, we combined these two methods and created hybrid wind turbine towers. These hybrid towers out-perform towers with only tapering effects or only bumpy surfaces. Test results prove that these two RCS mitigation strategies are not in mutual conflict. Instead, being put together, they produce additive effects on RCS reduction.

The taper ratio of a tower significantly influences its RCS. The higher the taper ratio, the lower the RCS. However, for a pragmatic tower, the taper ratio should be within a limit. Otherwise, the costs to build the tower would be too high. Taper bump towers possess effective RCS reduction capabilities for various radar frequencies and taper ratios. The performance of taper bamboo towers may deteriorate if the radar frequency exceeds four GHz and the taper ratio is larger than 1.0/60. However, in other cases, it is the best tower shape to reduce RCS.

The efficiencies of the taper tower and taper bamboo tower are not affected by radar polarization. On the other hand, the taper bump tower produces different bi-static RCS if we alter the polarization method. When the radar waves are horizontally polarized, its bi-static RCS are lower. However, this phenomenon is not obvious in the major back scattering directions.

Funding: This research was partially supported by the Ministry of Science and Technology, Taiwan.

Conflicts of Interest: The author declares no conflict of interest.

References

1. Matthews, J.C.G.; Sarno, C.; Herring, R. Interaction between radar systems and wind farms. In Proceedings of the Loughborough Antennas and Propagation Conference, Loughborough, UK, 17–18 March 2008; pp. 461–464.
2. Pinto, J.; Mathews, C.G.; Sarno, C. Radar signature reduction of wind turbines through the application of stealth technology. In Proceedings of the EuCAP Conference, Berlin, Germany, 23–27 March 2009; pp. 3886–3890.
3. Rashid, L.S.; Brown, A.K. Partial Treatment of Wind Turbine Blades with Radar Absorbing Materials (RAM) for RCS Reduction. In Proceedings of the Fourth EuCAP Conference, Barcelona, Spain, 12–16 April 2010; pp. 100–110.
4. Rashid, L.S.; Brown, A.K. Radar cross-section analysis of wind turbine blades with radar absorbing materials. In Proceedings of the European Radar Conference (EuRAD), Manchester, UK, 12–14 October 2011; pp. 97–100.
5. Ling, H.; Chou, R.-C.; Lee, S.-W. Shooting and Bouncing Rays: Calculating the RCS of an arbitrarily shaped cavity. *IEEE Trans. Antennas Propag.* **1989**, *37*, 194–205. [CrossRef]
6. Ueng, S.K.; Chan, Y.H. A Reshaping method for wind turbine RCS reduction. *Appl. Mech. Mater.* **2015**, *764*, 457–461. [CrossRef]
7. Ueng, S.K.; Chan, Y.H.; Lu, W.H.; Chang, H.W. Radar return reduction for wind turbines by using bump structures. *Sains Malays.* **2015**, *44*, 1701–1706.

8. Ueng, S.K.; Chen, Y.W. Scattering Reduction Using Bumps and Tapering Effect. In Proceedings of the ICCPE2016 Conference, Kenting, Taiwan, 30 September–3 October 2016.
9. Hou, Y.C.; Liao, W.J.; Ke, J.F.; Zhang, Z.C. Broadband and broad-angle dielectric-loaded RCS reduction structures. *IEEE Trans. Antennas Propag.* **2019**, *67*, 3334–3345. [CrossRef]
10. Song, J.; Wu, X.; Huang, C.; Yang, J.; Ji, C.; Zhang, C.; Luo, X. Broadband and tunable RCS reduction using high-order reflections and salisbury-type absorption mechanisms. *Sci. Rep.* **2019**, *9*, 9036. [CrossRef] [PubMed]
11. Chen, J.; Cheng, Q.; Zhao, J.; Dong, D.S.; Cui, T.J. Reduction of radar cross section based on a metasurface. *Prog. Electromagn. Res.* **2014**, *146*, 71–76. [CrossRef]
12. Mighani, M.; Dadashzadeh, G. Broadband RCS reduction using a novel double layer chessboard AMC surface. *Electron. Lett.* **2016**, *52*, 1253–1255. [CrossRef]
13. Baldauf, J.; Lee, S.W.; Lin, L.; Jeng, S.K. High frequency scattering from trihedral corner reflectors and other benchmark targets: SBR versus experiment. *IEEE Trans. Antennas Propag.* **1991**, *39*, 1345–1351. [CrossRef]